

Effective mass of helium atoms in one-dimensional microporous channels

B. Y. Chen, S. D. Mahanti, and M. Yussouff

*Department of Physics and Astronomy and Center for Fundamental Materials Research,
Michigan State University, East Lansing, Michigan 48824*

(Received 5 July 1994)

In microporous media characterized by a pore size in the range 5–15 Å, mass transport of He atoms at low temperatures is quantum mechanical in nature. By solving the one-particle Schrödinger equation, we investigate the effective mass m^*/m of He atoms (bare mass m) moving inside one-dimensional tubular channels consisting of cylindrical cages connected by necks of different diameters and lengths. We find that m/m^* is a highly nonlinear function of the geometrical parameters characterizing these channels. In certain cases, m/m^* changes rapidly from 1 to zero indicating the possibility of transition from delocalized to localized state. We also find that in the presence of attractive potential produced by positive ions located on the channel wall, the atoms are trapped near the wall, resulting in a drastic reduction in m/m^* .

I. INTRODUCTION

It is known that the physical properties of helium atoms (^3He , ^4He), when moving in restricted geometry, differ dramatically from those in the bulk, particularly at low temperatures, due to the influence of the topology of the confining medium and the adsorption potentials exerted by the medium on the He atoms. Typical examples are helium adsorbed on graphite^{1,2} and alkali-metal^{3,4} substrates, inside porous glass such as vycor^{5,6} or microporous media such as zeolites.^{7–15} In fact, recent sorption measurements¹⁶ of helium in fullerite crystals and films suggest that helium atoms might be mobile within the microporous space of these crystals, thus opening up the possibility of realizing a new type of three-dimensional quantum fluid.

One of the fundamental quantities that not only controls the mobility (transport), but also other physical properties such as heat capacity and magnetic susceptibility (through density of states and interaction effects) in a confining geometry is the effective mass (m^*/m) of He atoms. Depending upon the strength of the substrate potential and the nature of the microporous geometry, m^*/m can vary enormously. In particular, if the effective mass is large, any small perturbation such as coupling to the vibrational degrees of freedom of the confining medium, interparticle interaction or static disorder will tend to localize the particles, thus strongly affecting their transport and thermodynamic properties. Therefore, before one attempts to understand the effects of disorder (both structural and thermal) and interparticle interaction, one must understand the effect of periodic geometry on the motion of a single helium atom.

In this paper, we address the question of the effective mass of a single helium atom moving in one-dimensional microporous channels found in K-L zeolite,^{12,13} immodolite,¹⁷ etc. We study these systems primarily for two reasons. First, one-dimensional systems are relatively simple and second, extensive studies of low- T thermodynamic properties of ^3He and ^4He atoms in K-L zeolite

have been made¹² which we can address theoretically. K-L zeolite consists of one-dimensional channels of about 10 Å diameter modulated by constrictions (necks) of about 7 Å in diameter. Other one-dimensional zeolites in which helium adsorption studies have also been made are ZSM-23,^{14,15} whose diameter is ~ 5.5 Å. In principle, transport measurements can be made in these systems to directly probe the effective mass, but none appears to have been reported so far.

Physical systems for which our calculations of m/m^* are also relevant are electrons moving inside the narrow channels of electrides¹⁸ where the channels are formed in the space between large organic cage-like molecules encapsulating positive alkali ions. Electrides are an exciting new class of systems which exhibit a wide variety of electronic properties. Also recently, energy-band structures have been obtained by Lent and Leng¹⁹ for electrons moving inside periodically modulated channels, but these authors have not focused on the question of the effective mass which is of major interest here.

Figure 1(a) gives a schematic picture of K-L zeolite, whose channels consist of cages connected by neck regions. The boundary walls are formed by Si-O-Si networks. In K-L zeolite, some of the Si^{4+} ions are replaced by Al^{3+} ions and in addition there are charge compensating K^+ ions. Some of these K^+ ions are attached to the interior walls of the cage and the rest are embedded in the silicate framework. The K^+ ions on the wall provide an attractive potential on the helium atoms. Thus in addition to the geometrical confinement effects, the attractive potential produced by the K^+ ions can also affect m/m^* dramatically, particularly when the neck becomes narrow.

The arrangement of this paper is as follows. In Sec. II, we discuss in detail the parameters of the model system and briefly discuss the method of calculation of m/m^* . In Sec. III, we discuss our results on (a) size dependence of the ground-state energy, (b) m/m^* as a function of different geometrical parameters, and (c) the effect of attractive K^+ potential on m/m^* . Finally, in Sec. IV, we give a brief summary.

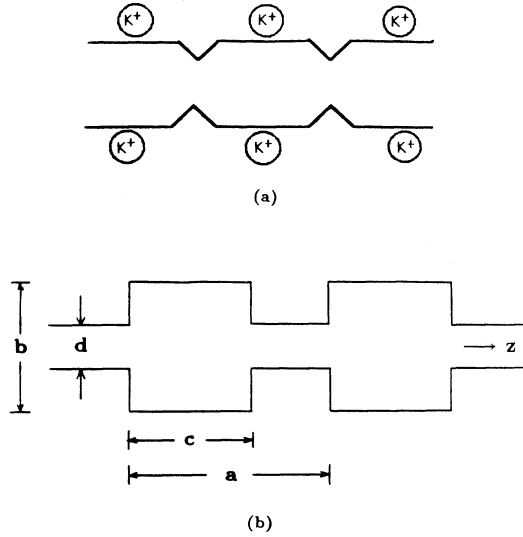


FIG. 1. (a) Schematic picture of a one-dimensional K-L zeolite tube; (b) Geometrical parameters describing the one-dimensional channel system.

II. SYSTEM AND METHOD

Figure 1(b) describes the geometrical parameters used in our one-dimensional (1D) model of the channel in K-L zeolite, it is periodic along the z axis with periodicity a . The channel consists of cages (chambers) of diameter b and length $0 \leq c \leq a$, connected by necks of diameter d and length $a - c$. The channel has cylindrical symmetry with the z axis as the symmetry axis. The transport properties of a quantum particle in such a channel is influenced both by the geometry and the potential. To examine exclusively the dependence of the transport properties (through m/m^*) on the geometry, we assume that the potential inside the channel is zero and the boundary is a hard wall where the wave function vanishes.

We solve the single-particle Schrödinger equation by setting the eigenfunctions as Bloch functions, $\psi_{n,m,k}(r, \phi, z) = u_{n,m,k}(r, \phi, z)e^{ikz}$. We then solve the equation for the cell periodic part $u_{n,m,k}$ and eigenvalues $E_{nm}(k)$. The numerical method used is the optimized iterative method for eigenvalue problems²⁰ for the simple 1D case, i.e., $\psi(r, \phi, z) \rightarrow \psi(z)$, with appropriate generalization to our problem. Using this method we can get eigenvalues and eigenvectors for the ground state and several low-lying excited states. To probe the effect of the dimensionality of the lateral (perpendicular to the tube axis) confinement, we have also studied the 2D case where $\psi(x, y, z) = \psi(x, z)$.

In this paper, we discuss only the lowest energy band for a fixed overall size of the channel [i.e., fixed a, b , shown in Fig. 1(b), but with different cage size c and neck diameter d]. Using this band structure and the effective-mass concept, i.e., assuming that $E = \hbar^2 k^2 / (2m^*) = (m/m^*)k^2(\hbar^2/2m)$ near the bottom of the energy band, we have calculated m/m^* . The unit of energy is $\hbar^2/(2m \text{ \AA}^2)$. For the one-dimensional channel, one can easily see that $m/m^* = 1$ when $c=0$ and/or $d=b$ which

corresponds to the propagation of a free particle along the z axis. Thus, if $m/m^* \approx 1$, the particle can move freely along the channel axis and if $m/m^* < 1$, the effective mass of the particle becomes large, i.e., the particle becomes heavier so that it is harder to move along the channel. As $m/m^* \rightarrow 0$, the particle has a tendency to get localized. In addition to m/m^* , we give the wave function densities (u^2) for $k=0$ to show what happens to the unit-cell wave functions as $m/m^* \rightarrow 0$. Finally, to see the effect of the K^+ ions, we have compared the difference between m/m^* for two cases, i.e., with and without the attractive potential produced by the K^+ ions.

III. RESULTS AND DISCUSSION

A. Effect of geometry on the energy spectrum and m/m^*

We will first present our results for fixed values of a and b and different values of cage length (c) and neck diameter (d). For simplicity, in this paper we choose $a=b$ and $a=10 \text{ \AA}$, we do not expect much qualitative change from our present results when we take $a \neq b$. Before discussing the geometry dependence of the effective mass, we would like to briefly discuss the size dependence of the energy itself, particularly the ground-state energy E_0 . We have calculated E_0 by changing the overall length scale (a) but keeping all the ratios b/a , c/a , d/a same and we find that E_0 scales as inverse square of a , as expected from elementary quantum mechanics.

In contrast to the ground-state energy, effective mass has a much more complex geometry dependence. In Fig. 2 we give the c dependence of m/m^* for three different values of d ($=3.5 \text{ \AA}$, 5.0 \AA , and 6.5 \AA) for the 2D case, and in Fig. 3 similar results are given for the tubular channel for two different values of d ($=3.66, 5.12 \text{ \AA}$). In all these calculations we have fixed $a=b=10 \text{ \AA}$. The general trend is as follows: For small c , $m/m^* \sim 1$. It decreases with increasing c and attains a minimum for $c \sim d$. Then it increases with increasing c . The decrease is quite sharp for the tubular channel when d is small. In this case, there is a large region of c for which $m/m^* \ll 1$ when d is small. Finally, when $c=a$ and $d < 10 \text{ \AA}$, m/m^* is less than 1 because in this limit the

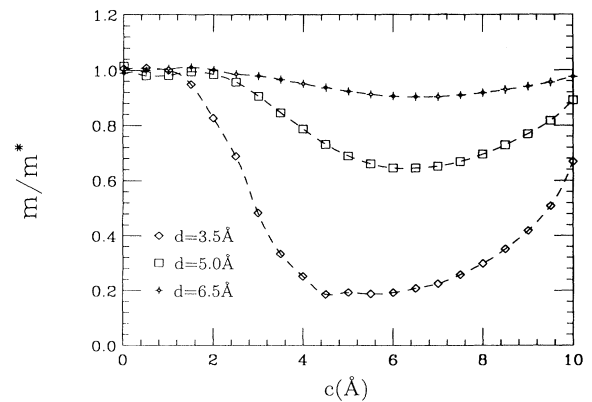


FIG. 2. The c dependence of m/m^* for three different neck diameters in the 2D case.

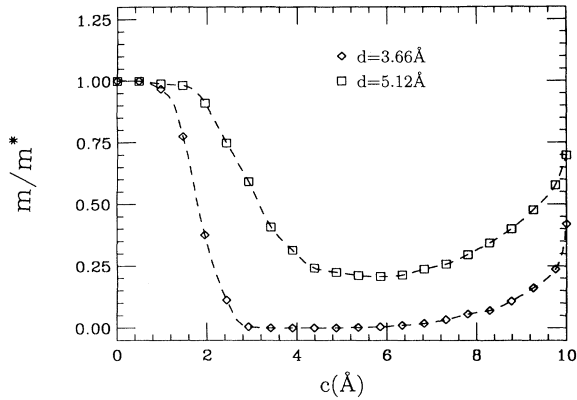


FIG. 3. The c dependence of m/m^* for two different neck diameters in the 3D, i.e., tubular channel case.

particle still feels the effect of geometry even if the neck length $\rightarrow 0$. In fact $m/m^* \rightarrow 1$ only when $d \rightarrow b = 10 \text{ \AA}$, in which case the particle moves freely inside a tube of uniform cross section.

To understand the physical origin of the sharp drop in m/m^* , i.e., enhanced tendency to localize as we increase the cage length c , we plot in Fig. 4 ($c = 2 \text{ \AA}$) and Fig. 5 ($c = 6 \text{ \AA}$) the square of the ground-state wave function ($k=0$) for the neck size $d = 3.5 \text{ \AA}$ for the 2D case. For $c = 2 \text{ \AA} < d$, $m/m^* \approx 1$ and the probability of the particle inside the neck region is quite high, whereas for $c = 6 \text{ \AA} > d$, most of the probability is in the cage with almost vanishing probability in the neck. In the latter case when we make $k \neq 0$, the k dependence of the energy comes from the small intercage tunneling process. This leads to a rather low value for m/m^* which for these parameter values is ≈ 0.19 .

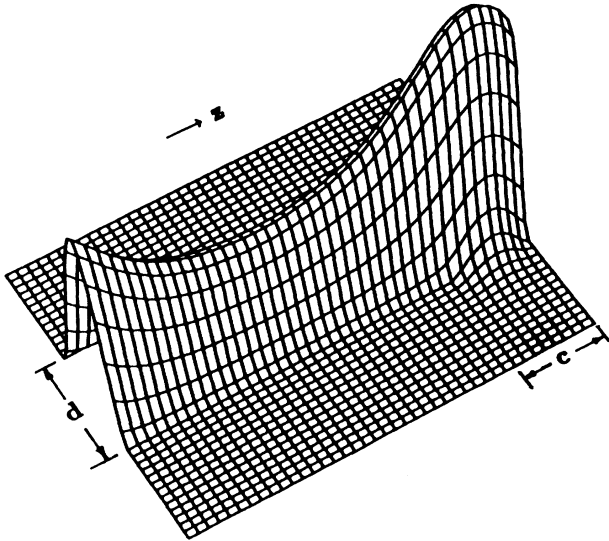


FIG. 4. Square of the wave function (u^2) of a particle moving in a channel for $k=0$ corresponding to the 2D case. The channel parameters are $a=b=10 \text{ \AA}$, $c=2.0 \text{ \AA}$, and $d=3.5 \text{ \AA}$. For these parameters, cage length is smaller than the neck diameter and m/m^* for this case $\approx 0.83 \approx 1$.

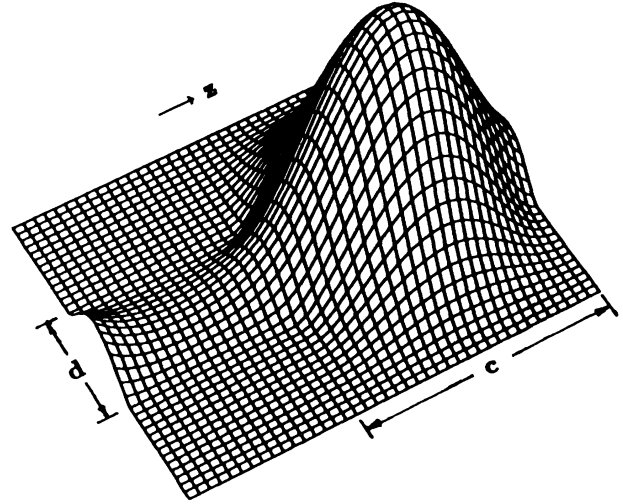


FIG. 5. Square of the wave function (u^2) of a particle moving in a channel for $k=0$, corresponding to the 2D case. The channel parameters are $a=b=10 \text{ \AA}$, $c=6.0 \text{ \AA}$, and $d=3.5 \text{ \AA}$. For these parameters, cage length is larger than the neck diameter and $m/m^* \approx 0.19 \ll 1$.

One can also study the above tendency to localize by changing d for fixed values of the cage length c . In Fig. 6, we give m/m^* as a function of d for three different values of c ($=2.5, 5.0, 7.5 \text{ \AA}$) for the tubular channel. For small values of d , $m/m^* \rightarrow 0$ but as we increase d , there is a rapid increase in m/m^* to 1. The sharpness of this increase depends on c , the increase being sharpest for small c . The value of d at which $m/m^* = 0.5$, initially increases with c but then tends to saturate at about 6 \AA .

B. Analytical fits to m/m^*

In order to express the geometry dependence of m/m^* in a simple analytical form, we have attempted to express (qualitatively) m/m^* as a function of scaled variables b/a , c/a , d/a . In our calculation, we have fixed $b/a=1$ and changed $0 < c/a, d/a < 1$. When d/a is small and c/a is large, one knows that $m/m^* \rightarrow 0$ exponentially as $d/a \rightarrow 0$ due to tunneling between the cage

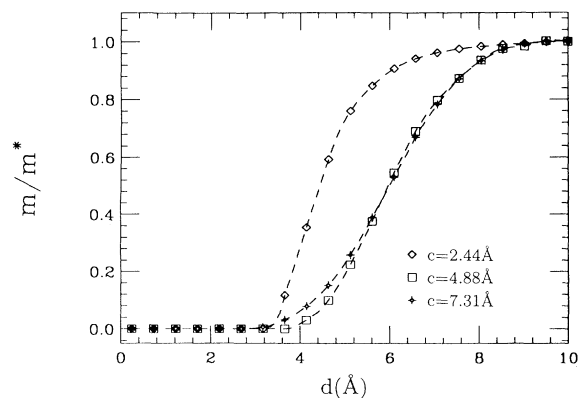


FIG. 6. m/m^* as a function of neck diameter d for three specific values of the cage length c .

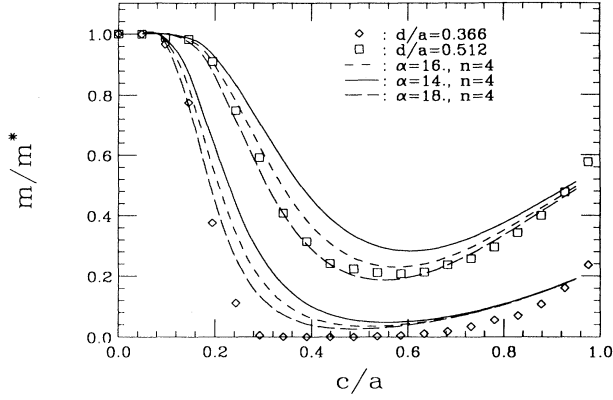


FIG. 7. Comparison between the two-parameter function [Eq. (1)] for m/m^* and the calculated m/m^* as a function of c/a for different values of d/a ; varying parameter α and fixing n .

states. But to capture the d/a , c/a dependence over a broad parameter space, we have used a different functional form. In fact, a two-parameter function that fits m/m^* data reasonably well is given by

$$\frac{m}{m^*} = 1 - \frac{[1 - \bar{d}\alpha\bar{c}(1 - \bar{d}\bar{c})]^{\alpha(1 - \bar{d}\bar{c})}}{1 + [(n/2)\bar{d}\bar{c}]^n}, \quad (1)$$

where $\bar{c} \equiv c/a$, $\bar{d} \equiv d/a$ and the two parameters are α and n .

In Fig. 7 we compare the results of Eq. (1) with the numerically calculated values of m/m^* as a function of \bar{c} for two different values of \bar{d} ($=0.366, 0.512$). We see that the parameter α controls the sharpness of the rapid decrease in m/m^* as \bar{c} increases from 0. For large values of \bar{c} , m/m^* is relatively insensitive to α . In Fig. 8, we give similar results but fix α and vary n . Clearly the m/m^* values depend sensitively on n as $\bar{c} \rightarrow 1$ and there is hardly any n dependence for $\bar{c} < 0.4$. The parameters which fit our calculated results well are $\alpha = 18$ and $n = 4$. One can obviously fit the data better by increasing the number of parameters but one does not necessarily gain any additional insight.

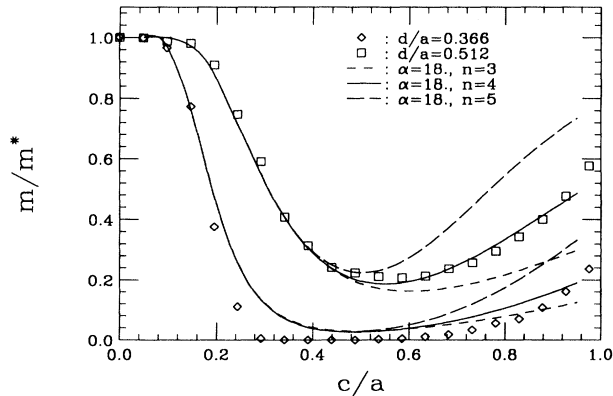


FIG. 8. Comparison between the two-parameter function [Eq. (1)] for m/m^* and the calculated m/m^* as a function of c/a for different values of d/a ; varying parameter n and fixing α .

C. Effects of attractive potential due to adsorbed ions on the cage surface

The nature of the attractive potential produced by the positive ions on the channel wall depends sensitivity on the location and number of positive ions inside the zeolite cage. As an example, let us discuss the case of K-L zeolite. Depending on the number of K^+ ions, there will be several minima as one goes around the wall of the cage. To represent the general features of this ion-induced attractive potential, we add a potential of the form

$$V(r, \phi, z) = \begin{cases} -V_0 \frac{r}{(b/2)} \sin^2(p\phi), & 0 < z < c \\ 0, & \text{otherwise.} \end{cases} \quad (2)$$

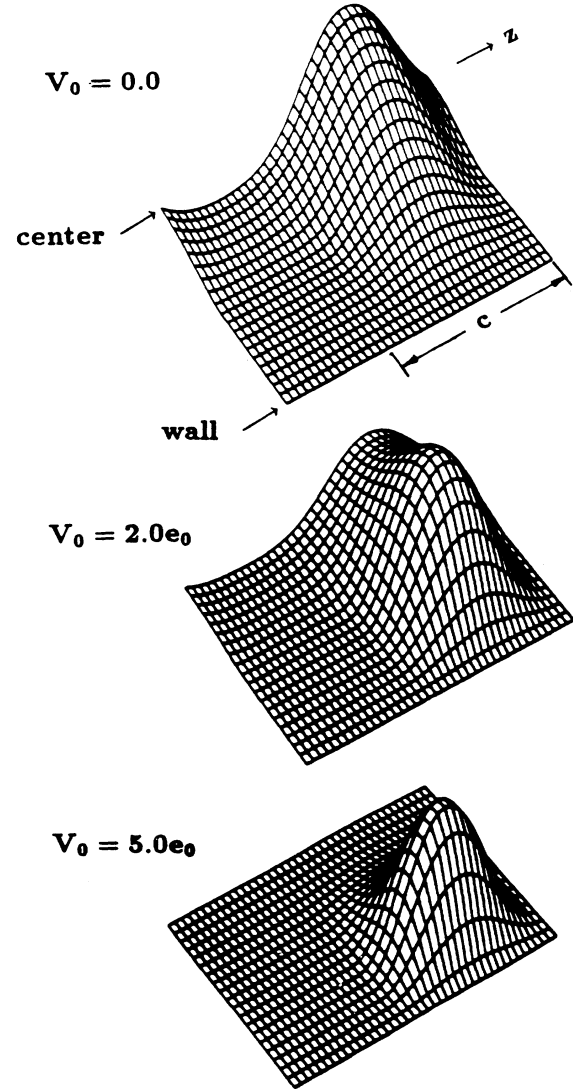


FIG. 9. Square of the wave function (u^2) at $k=0$. The channel parameters are $a=b=10 \text{ \AA}$, $c=6.0 \text{ \AA}$, and $d=5.0 \text{ \AA}$; (a) without the additional attractive potential ($V_0=0$) (b) with attractive potential, $V_0=2.0e_0$; (c) with attractive potential, $V_0=5.0e_0$. Here $e_0 = \hbar^2/(2m \text{ \AA}^2)$.

In the above r is the radial distance of the He atom from the axis of the tube, V_0 and p characterize, respectively, the strength and the angular periodicity of the attractive potential. Here we have assumed, for simplicity, that the K^+ ions do not affect the helium atoms when they are inside the neck region. In a more realistic model, one may have to relax this simplifying approximation.

To understand the effect of K^+ ions, we have chosen as before $a=b=10 \text{ \AA}$. We fix $c=6 \text{ \AA}$, $d=5 \text{ \AA}$, and take $p=2$ in Eq. (2). When $V_0=0$, $m/m^* \simeq 0.19$, when $V_0=2e_0$ ($e_0=\hbar^2/2m \text{ \AA}^2$), $m/m^* \simeq 0.06$ and when $V_0=5.0e_0$, $m/m^*=0.03$. Thus, an attractive potential produced by the cations located on the cage wall tends to increase the effective mass. The underlying physics is quite simple. When $V_0=0$, $m/m^* < 1$ indicating that intercage tunneling rate is small. As we turn on V_0 , the particles get attached towards the wall thus decreasing their intercage tunneling probability and hence decreasing m/m^* . As V_0 becomes sufficiently strong, the particles get trapped near the cage wall and do not contribute to the mass transport along the tube axis. However, these trapped particles can dominate the low- T thermodynamic properties, particularly at low He concentrations.

The square of wave function u^2 for $k=0$ is plotted in Fig. 9 for the three above values of V_0 . When $V_0=0$, the cage size is large enough such that the particles spend most of the time inside the cage ($m/m^*=0.19$). However, u^2 is reasonably large near the tube axis indicating an appreciable intercage tunneling probability. As we in-

crease V_0 , u^2 near the cage axis tends to decrease and for $V_0=5.0e_0$, the particle spends most of the time away from the tube axis, i.e., they are trapped near the cage walls. In this cage, intercage tunneling is practically zero. The excitations of these particles then come from tunneling around the cage wall, an intracage process.

IV. SUMMARY

In summary, we have investigated the effects of geometrical confinement on the effective mass m^*/m of quantum particles moving along tubular channels. We find that m^*/m is a highly nonlinear function of the geometrical parameters such as cage size c/a and/or neck diameter d/a . There are large regions of parameter values where the m^*/m is quite large. Consequently any small perturbations like defects, thermal vibration of the wall, or interparticle interaction will have strong effect on mass transport along the channel axis. The effect of positive ions embedded in the channel walls can also be very significant. In particular, in the low helium atom concentration regime, helium atoms will be trapped in states near the wall with an extremely low probability of intercage motion. These states will not contribute to mass transport but will show up in low-temperature thermal excitations.²¹

ACKNOWLEDGMENTS

This work was partially supported by NSF Grant No. CHE-9224102, and a grant from Ford Motor Company.

- ¹J. G. Dash, *Films on Solid Surfaces* (Academic, New York, 1975), Chap. 8; F. J. Milford and A. D. Novaco, *Phys. Rev. A* **4**, 1136 (1971).
- ²J. Yuyama, *J. Low Temp. Phys.* **47**, 1 (1982).
- ³E. Cheng, M. W. Cole, W. F. Saam, and J. Treiner, *Phys. Rev. Lett.* **67**, 1007 (1991).
- ⁴E. Cheng, M. W. Cole, J. Dupon-Roc, W. F. Saam, and J. Treiner, *Rev. Mod. Phys.* **65**, 557 (1993), and references therein.
- ⁵R. H. Tait and J. D. Reppy, *Phys. Rev. B* **20**, 997 (1980).
- ⁶B. C. Crooker, B. Hebral, E. N. Smith, Y. Takano, and J. D. Reppy, *Phys. Rev. Lett.* **51**, 666 (1983).
- ⁷N. Wade, T. Ito, and T. Watanabe, *J. Phys. Soc. Jpn.* **53**, 913 (1984).
- ⁸N. Wada, H. Kato, H. Shirataki, S. Takayanagi, T. Ito, and T. Watanabe, in *Proceedings of the 17th International Conference on Low Temperature Physics*, edited by U. Eckern, A. Schmid, W. Weber, and H. Wühl (North-Holland, Amsterdam, 1984), p. 521.
- ⁹H. Kato, N. Wada, T. Ito, S. Takayanagi, and T. Watanabe, *J. Phys. Soc. Jpn.* **55**, 246 (1986).
- ¹⁰N. Wade, Y. Yamamoto, H. Kato, T. Ito, and T. Watanabe, in *New Developments in Zeolite Science and Technology*, edit-

- ed by Y. Murakami, A. Iijima, and J. W. Ward (Kohdansha, Tokyo, 1986), p. 625.
- ¹¹N. Wade, K. Ishioh, and T. Watanabe, *J. Phys. Soc. Jpn.* **61**, 931 (1992).
- ¹²N. Wade, H. Kato, S. Sato, S. Takayanagi, T. Ito, and T. Watanabe, in *Proceedings of the 17th International Conference on Low Temperature Physics* (Ref. 8), p. 523.
- ¹³H. Kato, K. Ishioh, N. Wade, T. Ito, and T. Watanabe, *J. Low Temp. Phys.* **68**, 321 (1987).
- ¹⁴H. Deguchi, K. Konishi, K. Takeda, and N. Uryu, *Physica B* **165&166**, 571 (1990).
- ¹⁵K. Konishi, H. Deguchi, and K. Takeda, *J. Phys. Condens. Matter* **5**, 1619 (1993).
- ¹⁶C. P. Chen, S. Mehta, L. P. Fu, A. Petrou, F. M. Gasparini, and A. Hebard, *Phys. Rev. Lett.* **71**, 739 (1993).
- ¹⁷V. C. Farmer, M. J. Adams, A. R. Fraser, and F. Palmieri, *Clay Miner.* **17**, 459 (1983).
- ¹⁸M. J. Wagner, R. H. Huang, J. L. Eglin, and J. L. Dye, *Nature (London)* **368**, 726 (1994), and references therein.
- ¹⁹C. S. Lent and M. Leng, *App. Phys. Lett.* **58**, 1650 (1991).
- ²⁰S. E. Koonin, *Computational Physics* (Addison-Wesley, Reading, MA, 1986).
- ²¹B. Y. Chen, S. D. Mahanti, and M. Yussouff (unpublished).